

Origin of Jahn-Teller distortion and orbital-order in LaMnO₃

Eva Pavarini and Erik Koch

*Institut für Festkörperforschung and Institute for Advanced Simulation,
Forschungszentrum Jülich, 52425 Jülich, Germany*

(Dated: July 3, 2018)

The origin of the cooperative Jahn-Teller distortion and orbital-order in LaMnO₃ is central to the physics of the manganites. The question is complicated by the simultaneous presence of tetragonal and GdFeO₃-type distortions and the strong Hund's rule coupling between e_g and t_{2g} electrons. To clarify the situation we calculate the transition temperature for the Kugel-Khomskii superexchange mechanism by using the local density approximation+dynamical mean-field method, and disentangle the effects of super-exchange from those of lattice distortions. We find that super-exchange alone would yield $T_{KK} \sim 650$ K. The tetragonal and GdFeO₃-type distortions, however, reduce T_{KK} to ~ 550 K. Thus electron-phonon coupling is essential to explain the persistence of local Jahn-Teller distortions to $\gtrsim 1150$ K and to reproduce the occupied orbital deduced from neutron scattering.

PACS numbers: 71.10.Fd, 71.10.-w, 71.27.+a, 71.10.Hf, 71.30.+h

The insulating perovskite LaMnO₃ is the parent compound of the colossal magneto-resistance manganites [1] and it is considered a text-book example of a cooperative Jahn-Teller (JT) orbitally-ordered material [2]. Two distinct mechanisms have been proposed to explain the cooperative distortion: many-body Kugel-Khomskii (KK) super-exchange (SE) [3] and one-electron electron-phonon (EP) coupling [4]. Determining the relative strength of these mechanisms will provide a measure of the importance of strong correlation effects for the orbital physics in the manganites. Unfortunately the situation is complicated by the simultaneous presence of tetragonal and GdFeO₃-type distortions as well as a strong Hund's rule coupling between the Mn e_g and t_{2g} electrons.

In LaMnO₃ the Mn³⁺ ions are in a $t_{2g}^3 e_g^1$ configuration. Due to strong Hund's rule coupling the spin of the e_g electron is parallel to the spin of the t_{2g} electrons on the same site. Above $T_N = 140$ K the spins on neighboring sites are disordered [5]. The crystal structure is orthorhombic (Fig. 1). It can be understood by starting from an ideal cubic perovskite structure with axes \mathbf{x} , \mathbf{y} and \mathbf{z} : First, a tetragonal distortion reduces the Mn-O bond along \mathbf{z} by 2%. The La-O and La-Mn covalencies induce a GdFeO₃-type distortion [6, 7] resulting in an orthorhombic lattice with axes \mathbf{a} , \mathbf{b} , and \mathbf{c} , with the oxygen-octahedra tilted about \mathbf{b} and rotated around \mathbf{c} in alternating directions. Finally, the octahedra distort, with long (l) and short (s) bonds alternating along \mathbf{x} and \mathbf{y} , and repeating along \mathbf{z} [8–11]. This is measured by $\delta_{JT} = (l - s)/((l + s)/2)$. The degeneracy of the e_g orbitals is lifted and the occupied orbital, $|\theta\rangle = \cos\frac{\theta}{2}|3z^2 - 1\rangle + \sin\frac{\theta}{2}|x^2 - y^2\rangle$, is $\sim |3l^2 - 1\rangle$, i.e. it points in the direction of the long axis. Thus orbital-order (OO) is d -type with the sign of θ alternating along \mathbf{x} and \mathbf{y} and repeating along \mathbf{z} . At 300 K the JT distortion is substantial, $\delta_{JT} = 11\%$, and $\theta \sim 108^\circ$ was estimated from neutron scattering data [8]. Above $T_{OO} \sim 750$ K a strong reduction to $\delta_{JT} = 2.4\%$ was reported [8, 12], accompanied by a change in θ to $\sim 90^\circ$

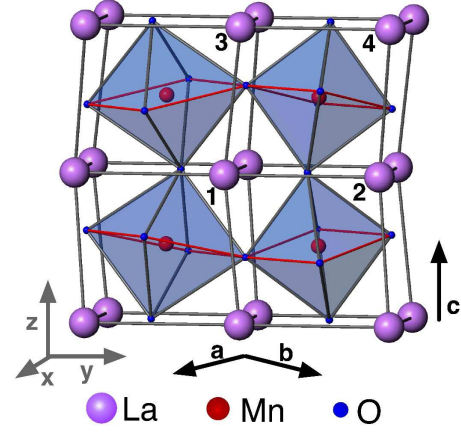


FIG. 1: (Color online) Structure of LaMnO₃ at 300 K [8]. The conventional cell is orthorhombic with axes \mathbf{a} , \mathbf{b} and \mathbf{c} , and contains 4 formula units. The pseudo-cubic axes (left corner) are defined via $\mathbf{a} = (\mathbf{x} - \mathbf{y})(1 + \alpha)$, $\mathbf{b} = (\mathbf{x} + \mathbf{y})(1 + \beta)$, and $\mathbf{c} = 2\mathbf{z}(1 + \gamma)$, with α, β, γ small numbers. For sites 1 and 3 the long (short) bond l (s) is \sim along \mathbf{y} (\mathbf{x}), vice versa for sites 2 and 4 (d -type pattern). All Mn sites are equivalent. The symmetries that transform them into a site of type 1 are: $x \leftrightarrow y$ (site 2) $z \rightarrow -z$ (site 3), $x \leftrightarrow y, z \rightarrow -z$ (site 4).

[8]. Recently this was, however, identified as an order-to-disorder transition [10, 11]: Due to orientational disorder, the crystal appears cubic on average, while, within nano-clusters, the MnO₆ octahedra remain fully JT distorted up to $T_{JT} \gtrsim 1150$ K [11].

Model calculations based on super-exchange alone can account for d -type order, but yield, for the classical ground state, $\theta \sim 90^\circ$ [13]. Models of electron-phonon coupling in simple cubic perovskites instead give $\sim 120^\circ$ [4]. To explain the observed $\sim 108^\circ$, one might thus conclude that both mechanisms are of similar importance [3]. Such models are lacking, however, a realistic description of the crystal and the calculated θ is sensitive to the choice of parameters [4, 14]. LDA+ U calculations yield

$\theta = 109^\circ$ and show that Coulomb repulsion is fundamental to stabilize the Jahn-Teller distortions in the ground state [15]. This might be taken as evidence that Kugel-Khomskii super-exchange is the dominant mechanism, and electron-phonon coupling, enhanced by electron localization [15, 16], merely helps. On the other hand, recent semiclassical many-body calculations for model cubic perovskites indicate that electron-phonon coupling is essential to explain orbital ordering above 300 K [17].

While it is not obvious how well LDA+ U or semiclassical approaches capture the many-body nature of the KK super-exchange, it seems clear that the inclusion of the real crystal structure is crucial [3, 6, 18, 19]. The tetragonal and GdFeO₃-type distortions result in a sizable narrowing of the e_g bands [6, 7, 20], likely changing the relative strength of super-exchange and electron-phonon coupling. Since, in the presence of a crystal-field, Coulomb repulsion suppresses orbital fluctuations [6, 21], they may even compete with SE and EP coupling. To identify the driving mechanism for orbital-order in LaMnO₃, it is thus mandatory to account for both the realistic electronic structure and many-body effects. To understand the mechanism one has to disentangle the contribution of KK super-exchange from that of the JT or the GdFeO₃-type and tetragonal distortions.

In this Letter, we do this by calculating directly the Kugel-Khomskii super-exchange transition temperature, T_{KK} , with and without tetragonal and GdFeO₃-type distortions. We adopt the method used successfully for KCuF₃ [21], based on local-density approximation + dynamical mean-field theory (LDA+DMFT) [22].

First, we calculate the electronic structure *ab-initio* using the N^{th} -order muffin-tin orbital method. Since the Hund's rule energy gain is larger than the e_g - t_{2g} crystal-field splitting, the t_{2g} bands are $\frac{1}{2}$ - and the e_g bands $\frac{1}{4}$ -filled; the three t_{2g} electrons behave as a spin $\mathbf{S}_{t_{2g}}$ and couple to the e_g electron via an effective magnetic field $h = JS_{t_{2g}}$. In the paramagnetic phase ($T > T_N = 140$ K) the t_{2g} spins are spatially disordered. The minimal model to study the KK mechanism in LaMnO₃ is thus [24]

$$\begin{aligned}
 H = & \sum_{im\sigma, jm'\sigma'} t_{m,m'}^{i,i'} u_{\sigma,\sigma'}^{i,i'} c_{im\sigma}^\dagger c_{jm'\sigma'} \\
 & - h \sum_{im} (n_{im\uparrow} - n_{im\downarrow}) + U \sum_{im} n_{im\uparrow} n_{im\downarrow} \\
 & + \frac{1}{2} \sum_{im(\neq m')\sigma\sigma'} (U - 2J - J\delta_{\sigma,\sigma'}) n_{im\sigma} n_{im'\sigma'} . \quad (1)
 \end{aligned}$$

$c_{im\sigma}^\dagger$ creates an electron with spin $\sigma = \uparrow, \downarrow$ in a Wannier orbital $|m\rangle = |x^2 - y^2\rangle$ or $|3z^2 - 1\rangle$ at site i , and $n_{im\sigma} = c_{im\sigma}^\dagger c_{im\sigma}$. \uparrow (\downarrow) indicates the e_g spin parallel (antiparallel) to the t_{2g} spins (on that site). The matrix u ($u_{\sigma,\sigma'}^{i,i'} = 2/3$ for $i \neq i'$, $u_{\sigma,\sigma'}^{i,i} = \delta_{\sigma,\sigma'}$) accounts for the orientational disorder of the t_{2g} spins [24]; $t_{m,m'}^{i,i'}$ is the LDA hopping integral from orbital m on site i to

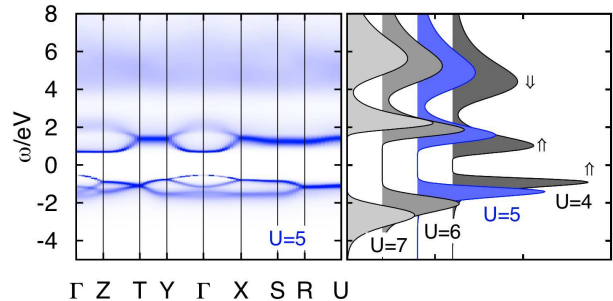


FIG. 2: (Color online) Right: LDA+DMFT spectral function for the room temperature structure R₁₁ for different U . \uparrow (\downarrow) indicates states with e_g spins parallel (antiparallel) to $\mathbf{S}_{t_{2g}}$. Left: \mathbf{k} -resolved spectral function for $U = 5$ eV.

orbital m' on site i' , obtained *ab-initio* by down-folding the LDA bands and constructing a localized e_g Wannier basis. The on-site terms $i = i'$ give the crystal-field splitting. U and J are the direct and exchange screened on-site Coulomb interaction [25]. We use the theoretical estimate $J = 0.75$ eV [26] and vary U between 4 and 7 eV. The Hund's rule splitting was estimated *ab-initio* to $2JS_{t_{2g}} \sim 2.7$ eV [7]. We solve (1) using DMFT [27] or cellular DMFT (CDMFT) and a quantum Monte Carlo [28] solver, working with the full self-energy matrix $\Sigma_{mm'}$ in orbital space [6]. The spectral matrix on the real-axis is obtained by analytic continuation [29].

We consider several structures: (i) the room temperature structure, R₁₁ with $\delta_{JT} = 11\%$, and a series of hypothetical structures, R $_{\delta_{JT}}$, with reduced JT distortion δ_{JT} , (ii) the (average) structure found at 800 K, R $_{2,4}^{800K}$, which has a slightly larger volume than R₁₁ and a smaller GdFeO₃-type distortion, and (iii) the ideal cubic structure, I₀, with the same volume as R₁₁. For all structures we find that at each site the e_g spins align to $\mathbf{S}_{t_{2g}}$. We calculate the orbital polarization p as a function of temperature [30] by diagonalizing the DMFT (or CMDFT) occupation matrix and taking the difference between the occupation of the most ($|\theta\rangle$) and least ($|\theta + \pi\rangle$) filled orbital. To test the t_{2g} spins picture we perform calculations for the 5-band ($e_g + t_{2g}$) Hubbard model [23]. We find that it holds even at high temperatures.

For the 300 K structure (R₁₁) the band-widths are $W_{t_{2g}} \sim 1.6$ eV and $W_{e_g} \sim 3.0$ eV. The e_g states split by ~ 840 meV, in good agreement with experimental estimates [31]. The lower crystal-field state at site 1 is $|1\rangle = 0.574|3z^2 - 1\rangle + 0.818|x^2 - y^2\rangle$. We find an insulating solution in the full range $U = 4 - 7$ eV (Fig. 2). The Mott gap E_g is ~ 0.6 eV for $U = 4$ eV, and increases almost linearly with increasing U . For $U = 5$ eV, suggested by recent estimates [7, 32], the Hubbard bands are at ~ -1.5 and 2 eV. In addition there is a broad feature around 5 eV due to e_g states with spin antiparallel to the randomly oriented t_{2g} spins. These spectra are

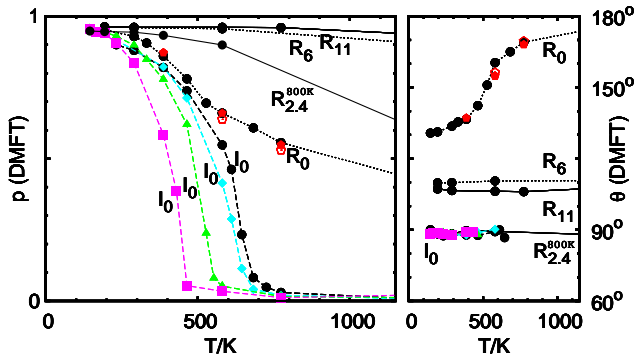


FIG. 3: (Color online) Orbital polarization p (left) and (right) occupied state $|\theta\rangle$ ($|\theta\rangle$) for sites 1 and 3 (2 and 4) as a function of temperature. Solid line: 300 K (R_{11}) and 800 K ($R_{2.4}^{800K}$) structures. Dots: orthorhombic structures with half (R_6) or no (R_0) Jahn-Teller distortion. Pentagons: 2 (full) and 4 (empty) sites CDMFT. Dashes: ideal cubic structure (I_0). Circles: $U = 5$ eV. Diamonds: $U = 5.5$ eV. Triangles: $U = 6$ eV. Squares: $U = 7$ eV. Crystal-field splitting (meV): 840 (R_{11}), 495 (R_6), 219 (R_0), 168 ($R_{2.4}^{800K}$), and 0 (I_0).

in line with experiments [31–34]. We find that even at 1150 K the system is fully orbitally polarized ($p \sim 1$). On sites 1 and 3, the occupied state is $|\theta\rangle \sim |106^\circ\rangle$, on sites 2 and 4 it is $|\theta\rangle \sim |106^\circ\rangle$ (d -type OO); $|\theta\rangle$ is close to the lower crystal-field state obtained from LDA (table I) and in excellent agreement with neutron diffraction experiments [8]. We find that things hardly change when the JT distortion is halved (R_6 structure in Fig. 3). Even for the average 800 K structure ($R_{2.4}^{800K}$) OO does not disappear: Although the Jahn-Teller distortion is strongly reduced to $\delta_{JT} = 2.4\%$, the crystal-field splitting is ~ 168 meV and the orbital polarization at 1150 K is as large as $p \sim 0.65$, while θ is now close to 90° . For all these structures, orbital order is already determined by the distortions via the crystal-field splitting.

To find the temperature T_{KK} at which Kugel-Khomskii super-exchange drives orbital-order we consider the zero crystal-field limit, i.e. the ideal cubic structure, I_0 . The e_g band-width increases to $W_{e_g} \sim 3.7$ eV and for $U = 5$ eV the system is a Mott insulator with a tiny gap only below $T \sim 650$ K. We find $T_{KK} \sim 650$ K, very close to the metal-insulator transition (Fig. 3). To check how strongly T_{KK} changes when the gap opens, we increase U . For $U = 5.5$ eV we find an insulating solution with a small gap of ~ 0.5 eV and T_{KK} still close to ~ 650 K. For $U = 6$ eV, $E_g \sim 0.9$ eV and $T_{KK} \sim 550$ K. Even with an unrealistically large $U = 7$ eV, giving $E_g \sim 1.8$ eV, T_{KK} is still as large as ~ 470 K. Thus, despite the small gap, T_{KK} decreases as $\sim 1/U$, as expected for super-exchange. For a realistic $U \sim 5$ eV, the calculated $T_{KK} \sim 650$ K is surprisingly close to the order-disorder transition temperature, $T_{OO} \sim 750$ K, though still much smaller than $T_{JT} \gtrsim 1150$ K. The occupied state at site 1 is $|\theta\rangle \sim$

$|90^\circ\rangle$ for all U .

Such a large T_{KK} is all the more surprising when compared with the value obtained for $KCuF_3$, $T_{KK} \sim 350$ K [21]. For the ideal cubic structure the hopping matrix (table I) is $t_{m,m'}^{i,i\pm z} \sim -t\delta_{m,m'}\delta_{m,3z^2-1}$, $t_{m,m}^{i,i\pm x} = t_{m,m}^{i,i\pm y} \sim -t/4(1 + 2\delta_{m,x^2-y^2})$, and for $m \neq m'$ $t_{m,m'}^{i,i\pm x} = -t_{m,m'}^{i,i\pm y} \sim \sqrt{3}t/4$. Since the effective (after averaging over the directions of $S_{t_{2g}}$) hopping integral in $LaMnO_3$, $2t/3 \sim 345$ meV is $\sim 10\%$ smaller than $t \sim 376$ meV in $KCuF_3$ [21], one may expect a slightly smaller T_{KK} in $LaMnO_3$, opposite to what we find. Our result can, however, be understood in super-exchange theory. The KK SE part of the Hamiltonian, obtained by second-order perturbation theory in t from Eq. (1), may be written as

$$H_{SE}^{i,i'} \sim \frac{J_{SE}}{2} \sum_{\langle ii' \rangle_{\mathbf{x},\mathbf{y}}} \left[3T_i^x T_{i'}^x \mp \sqrt{3} (T_i^z T_{i'}^x + T_i^x T_{i'}^z) \right] + \frac{J_{SE}}{2} \sum_{\langle ii' \rangle_{\mathbf{x},\mathbf{y}}} T_i^z T_{i'}^z + 2J_{SE} \sum_{\langle ii' \rangle_{\mathbf{z}}} T_i^z T_{i'}^z, \quad (2)$$

where $\langle i, i' \rangle_{\mathbf{x},\mathbf{y}}$ and $\langle i, i' \rangle_{\mathbf{z}}$ indicate near neighboring sites along \mathbf{x} , \mathbf{y} , or \mathbf{z} ; $-(+)$ refers to the \mathbf{x} (\mathbf{y}) direction, T_i^x and T_i^z are pseudospin operators [3], with $T_i^z |3z^2 - 1\rangle = 1/2 |3z^2 - 1\rangle$, $T_i^z |x^2 - y^2\rangle = -1/2 |x^2 - y^2\rangle$. The superexchange coupling is $J_{SE} = (\bar{t}^2/U)(w/2)$, where \bar{t} is the effective hopping integral. In the large U limit (negligible J/U and h/U), $w \sim 1 + 4\langle S_i^z \rangle \langle S_{i'}^z \rangle + (1 - 4\langle S_i^z \rangle \langle S_{i'}^z \rangle) u_{\uparrow,\downarrow}^{i,i'} / u_{\uparrow,\uparrow}^{i,i'}$, where S_i^z are the e_g spin operators. In $LaMnO_3$ the e_g spins align with the randomly oriented t_{2g} spins, thus $\bar{t} = 2t/3$, $w \sim 2$, and $J_{SE} \sim 2(2t/3)^2/U$. For d -type order, the classical ground-state is $|\theta\rangle \sim |90^\circ\rangle$, in agreement with our DMFT results. In $KCuF_3$, with configuration $t_{2g}^6 e_g^3$, the Hund's rule coupling between e_g and t_{2g} plays no role, i.e. $\langle S_i^z \rangle = 0$. The hopping integral $\bar{t} = t$ is indeed slightly larger than in $LaMnO_3$, but $w \sim 1$, a reduction of 50%. Consequently, J_{SE} is reduced by ~ 0.6 in $KCuF_3$. For finite J/U and h/U , w is a more complicated function, but the conclusions stay the same. We verified solving (1) with LDA+DMFT that also for $LaMnO_3$ T_{KK} drops drastically if $u_{\sigma,-\sigma}^{i,i'} = 0$ and $h = 0$.

It remains to evaluate the effect of the orthorhombic distortion on the transition. For this we perform calculations for the system R_0 with no Jahn-Teller distortion, but keeping the tetragonal and $GdFeO_3$ -type distortion of the 300 K structure. This structure is metallic for $U = 4$ eV; for $U = 5$ eV it has a gap of ~ 0.5 eV. We find a large polarization already at 1150 K ($p \sim 0.45$). Such polarization is due to the crystal-field splitting of about 219 meV, with lower crystal-field states at site 1 given by $|1\rangle \sim |x^2 - y^2\rangle$. Surprisingly the most occupied state $|\theta\rangle$ is close to $|1\rangle$ ($\theta \sim 180$) only at high temperature (~ 1000 K). The orthorhombic crystal-field thus competes with super-exchange, analogous to an external field with a component perpendicular to an easy axis. On cooling the occupied orbitals rotate to $|\theta\rangle \sim |132^\circ\rangle$

lmn	$t_{\pi,\pi}^{i,i'}$	$t_{\pi,0}^{i,i'}$	$t_{0,\pi}^{i,i'}$	$t_{0,0}^{i,i'}$	$t_{\pi,\pi}^{i,i'}$	$t_{\pi,0}^{i,i'}$	$t_{0,\pi}^{i,i'}$	$t_{0,0}^{i,i'}$
	R ₁₁				R _{2,4} ^{800K}			
000	0	409	409	305	0	84	84	-2
001	-8	-47	-47	-445	-2	-13	-13	-439
010	-322	233	174	-129	-328	196	190	-105
100	-322	-174	-236	-129	-328	-190	-196	-105
	R ₀				I ₀			
000	0	5	5	218	0	0	0	0
001	-1	-2	-2	-433	-10	0	0	-518
010	-333	206	207	-121	-391	220	220	-137
100	-333	-207	-206	-121	-391	-220	-220	-137

TABLE I: Hopping integrals $t_{m,m'}^{i,i'}/\text{meV}$ from a site i of type 1 to a neighboring site i' of type 2 in direction $lx + ny + mz$ for structures R₁₁, R_{2,4}^{800K}, R₀ and I₀. The states m, m' are $|\pi\rangle = |x^2 - y^2\rangle$ and $|0\rangle = |3z^2 - 1\rangle$. The crystal-field states are the eigenvectors of the on-site matrix ($l = m = n = 0$).

(see Fig. 3). This effect of super-exchange, occurs around a characteristic temperature $T_{\text{KK}}^{\text{R}} \sim 550$ K; still surprisingly large, but reduced compared to T_{KK} for the ideal cubic system I₀ and much smaller than the experimental $T_{\text{JT}} \gtrsim 1150$ K. Short-range correlations could reduce T_{KK}^{R} or modify θ . To estimate this effect we perform CDMFT calculations; our results (Fig. 3) remain basically unchanged. Thus, electron-phonon coupling is necessary to explain both the transition temperature and the correct occupied orbital $|\theta\rangle \sim |108^\circ\rangle$.

In conclusion, we find that T_{KK}^{R} in orthorhombic LaMnO₃ is ~ 550 K. We have shown that two elements are crucial: the super-exchange mechanism, which yields a transition temperature as high as 650 K, and the tetragonal plus GdFeO₃-type distortion, which, due to the reduced hopping integrals and the competing orthorhombic crystal-field, reduces T_{KK} to 550 K. Experimentally, an order-to-disorder transition occurs around $T_{\text{OO}} \sim 750$ K, but a local Jahn-Teller distortion persists in the disordered phase up to $T_{\text{JT}} \gtrsim 1150$ K. The Kugel-Khomskii mechanism alone cannot account for the presence of such Jahn-Teller distortions above 550 K ($T_{\text{KK}}^{\text{R}} \ll T_{\text{JT}}$). It also cannot justify the neutron scattering estimate $\theta = 108^\circ$. Thus electron-phonon coupling is a crucial ingredient, both for making the Jahn-Teller distortions energetically favorable at such high temperatures and in determining the occupied orbital.

We acknowledge discussions with D.I. Khomskii and A.I. Lichtenstein, and grant JIFF22 on Jugene.

[1] Y. Tokura and N. Nagaosa, *Science* **288**, 462 (2000).
[2] P. Fazekas, *Lecture Notes on Electron Correlation and Magnetism*, World Scientific, 1999.
[3] K.I. Kugel and D.I. Khomskii, *Zh. Eksp. Teor. Fiz.* **64**,

1429 (1973) [*Sov. Phys. JETP* **37**, 725 (1973)].
[4] J. Kanamori, *J. Appl. Phys.* **31**, S14 (1960).
[5] E.O. Wollan and W.C. Koehler, *Phys. Rev.* **100**, 545 (1955).
[6] E. Pavarini *et al.*, *Phys. Rev. Lett.* **92**, 176403 (2004); M. De Raychaudhury, E. Pavarini, O. K. Andersen, *ibid.* **99**, 126402 (2007); E. Pavarini, A. Yamasaki, J. Nuss and O.K. Andersen, *New J. Phys.* **7** 188 (2005).
[7] A. Yamasaki *et al.*, *Phys. Rev. Lett.* **96**, 166401 (2006).
[8] J. Rodríguez-Carvajal *et al.*, *Phys. Rev. B* **57**, R3189 (1998).
[9] T. Chatterji *et al.*, *Phys. Rev. B* **68**, 052406 (2003).
[10] M.C. Sánchez, G. Subías, J. García, and J. Blasco, *Phys. Rev. Lett.* **90**, 045503 (2003).
[11] X. Qiu, Th. Proffen, J.F. Mitchell, and S.J.L. Billinge, *Phys. Rev. Lett.* **94**, 177203 (2005); A. Sartbaeva *et al.*, *ibid.* **99**, 155503 (2007).
[12] Y. Murakami *et al.*, *Phys. Rev. Lett.* **81**, 582 (1998).
[13] J. Bała and A.M. Oleś, *Phys. Rev. B* **62**, R6085 (2000).
[14] R. Maezono, S. Ishihara, and N. Nagaosa, *Phys. Rev. B* **58**, 11583 (1998).
[15] W.G. Yin, D. Volja, and W. Ku, *Phys. Rev. Lett.* **96**, 116405 (2006).
[16] E. Koch and E. Pavarini, to be published.
[17] C. Lin and A.J. Millis, *Phys. Rev. B* **78**, 174419 (2008).
[18] T. Hotta, S. Yunoki, M. Mayr, and E. Dagotto, *Phys. Rev. B* **60**, R15009 (1999).
[19] L. E. Gonchar' and A. E. Nikiforov, *Fiz. Tverd. Tela* **42**, 1038 (2000) [*Phys. Solid State*, **42**, 1070 (2000)].
[20] C. Ederer, C. Lin, and A. J. Millis, *Phys. Rev. B* **76**, 155105 (2007).
[21] E. Pavarini, E. Koch, and A.I. Lichtenstein, *Phys. Rev. Lett.* **101**, 266405 (2008).
[22] V.I. Anisimov *et al.*, *J. Phys. Condensed Matter* **9**, 7359 (1997); A.I. Lichtenstein and M.I. Katsnelson, *Phys. Rev. B* **57**, 6884 (1998).
[23] Structure R₁₁, parameters $1/k_{\text{BT}} = 5$ eV, $U = 5$ eV, $J = 0.75$ eV. We find $\sim t_{2g}^3 e_g^2$ and Hubbard bands in line with $S_{t_{2g}} = 3/2$; the e_g orbital polarization, p and the gap are close to the results for Hamiltonian (1).
[24] K.H. Ahn, A.J. Millis, *Phys. Rev. B* **61**, 13545 (2000).
[25] J. Kanamori, *Prog. Theor. Phys.* **30**, 275 (1963).
[26] T. Mizokawa and A. Fujimori, *Phys. Rev. B* **54**, 5368 (1996).
[27] A. Georges, G. Kotliar, W. Kraut, M.J. Rozenberg, *Rev. Mod. Phys.* **68**, 13 (1996).
[28] J.E. Hirsch and R.M. Fye, *Phys. Rev. Lett.* **56**, 2521 (1986).
[29] J.E. Gubernatis, M. Jarrell, R.N. Silver and D.S. Sivia, *Phys. Rev. B* **44**, 6011 (1991).
[30] With e_g spins aligned to the t_{2g} spins, the SE coupling (see discussion after Eq. 2) is $J_{\text{SE}} \sim 2\bar{t}^2(1/(U - 3J) + (u_{\uparrow,\downarrow}/u_{\uparrow,\uparrow}))(1/(U + 2h - 2J) - 1/(U + 2h))$, i.e. depends weakly on the $u_{\sigma-\sigma}^{i,i'}$ terms in (1); thus we neglect them.
[31] N.N. Kovaleva *et al.*, *Phys. Rev. Lett.* **93**, 147204 (2004).
[32] J.-H. Park *et al.*, *Phys. Rev. Lett.* **76**, 4215 (1996).
[33] K. Takenaka *et al.*, *J. Phys. Soc. Jap.* **68**, 1828 (1999); J. H. Jung *et al.*, *Phys. Rev. B* **57**, R11043 (1998); M.A. Quijada *et al.*, *ibid.* **64**, 224426 (2001); K. Tobe *et al.*, *ibid.* **64**, 184421 (2001).
[34] A. Chainani, M. Mathew, and D.D. Sarma, *Phys. Rev. B* **47**, 15397 (1993); T. Saitoh *et al. ibid.* **51**, 13942 (1995); T. Saitoh *et al. ibid.* **56**, 8836 (1997).